molecular pharmaceutics

Article

Cite This: Mol. Pharmaceutics 2019, 16, 1606−1619

pubs.acs.org/molecularpharmaceutics

Minocycline and Silver Dual-Loaded Polyphosphoester-Based Nanoparticles for Treatment of Resistant *Pseudomonas aeruginosa*

Qingquan Chen,[†,∥] Kush N. Shah,[†,∥] Fuwu Zhang,[‡,∥] Adam J. Salazar,[§] Parth N. Shah,[†] Richen Li,[‡] James C. Sacchettini,*[,§] Karen L. Wooley,*[,‡] and Carolyn L. Cannon*[,†]

[†]Department of Microbial Pathogenesis and Immunology, Texas A&M Health Science Center, College Station, Texas 77843, United States

[‡]Department of Chemistry, Department of Chemical Engineering, Department of Materials Science and Engineering, and Laboratory for Synthetic-Biologic Interactions, Texas A&M University, College Station, Texas 77842, United States

[§]Department of Biochemistry and Biophysics, Texas A&M University, College Station, Texas 77842, United States

Supporting Information

ABSTRACT: *Pseudomonas aeruginosa* has been detected in the lungs of ∼50% of patients with cystic fibrosis (CF), including 20% of adult CF patients. The majority of these adult patients harbor multi-drug resistant (MDR) strains, limiting the available treatment options. Silver has long been used as a broad-spectrum antimicrobial agent with a low incidence of resistance. Despite low toxicity, poor availability of silver cations mandates a high dosage to effectively eradicate infections. To address this shortcoming of silver, nanoparticles have been used as delivery devices to improve treatment outcomes. Furthermore, studies have demonstrated that synergistic combinations with careful dose calibrations and efficient delivery systems result in superior antimicrobial activity while avoiding potential side effects of both therapeutics. Here 4-epi-minocycline, a metabolite of minocycline, was identified as an active antimicrobial against *P. aeruginosa* using a high-throughput screen. The antimicrobial activities of 4-epi-minocycline, minocycline, and silver acetate against clinical isolates of *P. aeruginosa* obtained from CF patients were evaluated in vitro. Next, the synergistic activity of the silver/minocycline combination against *P. aeruginosa* isolates was investigated using checkerboard assays and identified with end-point colony forming unit determination assays. Finally, nanoparticles coloaded with minocycline and silver were evaluated in vitro for antimicrobial activity. The results demonstrated that both silver and minocycline are potent antimicrobials alone and that the combination allows a reduced dosage of both therapeutics to achieve the same antimicrobial effect. Furthermore, the proposed synergistic silver/minocycline combination can be coloaded into nanoparticles as a next-generation antibiotic to combat the threats presented by MDR pathogens.

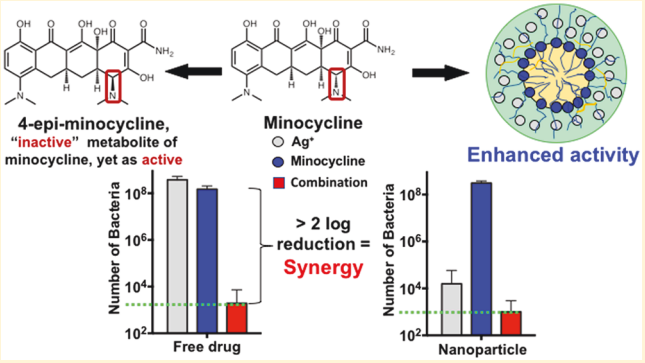

KEYWORDS: *P. aeruginosa, silver (Ag^+), 4-epi-minocycline, minocycline, synergy, nanoparticles*

INTRODUCTION

Pseudomonas aeruginosa is an opportunistic pathogen that causes complicated disease states such as bacteremia, otitis, and soft tissue, urinary tract, and respiratory infections. The overuse of antimicrobials and the lack of antibiotic stewardship programs has led to the development of resistance against several FDA-approved standard-of-care (SoC) therapeutics, including ciprofloxacin, levofloxacin, cefepime, and gentamicin.[1] Multi-drug resistant (MDR) *P. aeruginosa* has been designated as a "serious" threat by the Centers for Disease Control and Prevention (CDC).[2] With over 51 000 healthcare-associated infections, including 6700 MDR *P. aeruginosa* infections annually in the United States, *P. aeruginosa* is the leading cause of nosocomial infections and the second most common pathogen associated with ventilator-associated pneumonia (VAP).[3] *P. aeruginosa* infections are particularly challenging to manage and often result in poor prognosis for immunocompromised patients and patients with cystic fibrosis (CF). An estimated 47.5% of CF patients harbor *P. aeruginosa* in their lungs, including 9.2% of them with MDR *P. aeruginosa*.[4] In CF patients, the presence of sticky dehydrated mucus in the airways provides ideal conditions for the colonization of such opportunistic pathogens.[5,6] These pathogens in the accumulated mucus also form biofilms,[6] creating unique conditions resulting in poor drug penetration, ultimately leading to treatment failure despite the use of aggressive antibiotics.[7,8] Consequently, these chronic pulmo-

Received: December 11, 2018
Revised: February 25, 2019
Accepted: February 28, 2019
Published: February 28, 2019

DOI: 10.1021/acs.molpharmaceut.8b01288
Mol. Pharmaceutics 2019, 16, 1606−1619

nary infections result in declining lung function, which is the leading cause of mortality in CF patients.[6] Moreover, the repeated intravenous (i.v.) administration of high-dose antibiotics may result in severe side effects and increased propensity of resistance acquisition.[9,10] In addition to *P. aeruginosa*, several other pathogens reside in the CF lung[4] including *Staphylococcus aureus*, *Stenotrophomonas maltophilia*, and *Burkholderia cepacia* complex. According the CF patient registry, an estimated 71.1% of CF patients are colonized with *Staphylococcus aureus*, including 26% of patients colonized with methicillin-resistant *Staphylococcus aureus* (MRSA). MRSA has also been designated as a "serious" threat[2] and is another common perpetrator responsible for the deterioration of the CF lung. Thus to address the polymicrobial infection affecting this disease state, it is imperative to develop broad-spectrum therapeutics with potent antimicrobial activity against both Gram-positive and Gram-negative pathogens. Thus a combinatorial antimicrobial approach is particularly attractive to address polymicrobial infections.

Silver (Ag^+) is a broad-spectrum antimicrobial with multiple mechanisms of action, including its ability to condense bacterial DNA and disrupt bacterial cell membranes.[11] These diverse mechanisms provide potent antimicrobial activity[12] and may explain the paucity of reported cases of resistance[13−16] despite its widespread use to treat burn and wound infections.[17−21] Potent antimicrobial activity coupled to low toxicity to human tissues[22] has led to several FDA-approved antimicrobial dressings, such as Acticoat Absorbent, Actisorb Silver 220, and Aquacel Ag, with ionic silver as the active antimicrobial agent.[23] However, because of the affinity of silver cations for thiolated proteins or chloride ions,[24,25] the bioavailability of silver is poor, which suppresses the antimicrobial activity of silver ions,[25] necessitating an increased dosage to effectively eradicate infections. This shortcoming can be addressed through the use of efficient delivery systems such as nanoparticles. Several reports, including those by our research group, have demonstrated improved clinical outcomes when infections are treated with nanoparticle devices.[26] These improvements in treatment outcomes are often achieved with reduced drug dosages and fewer side effects compared with unencapsulated drug treatments. The high localized therapeutic concentrations achieved by nanoparticles often overwhelm drug-resistance mechanisms in pathogens, thereby improving the antimicrobial efficacy against drug-resistant pathogens.[27] Through the use of engineered nanoparticles, many antimicrobial agents with poor solubility, unfavorable pharmacokinetics, or poor penetration into diseased tissues can be successfully delivered at optimal therapeutic concentrations to eradicate MDR pathogens.[28,29]

We have previously demonstrated the ability of nondegradable and degradable nanoparticle formulations to shield silver from biological inactivation.[29,30] For example, shell-cross-linked knedel-like (SCK) nanoparticles exhibit comparable antimicrobial efficacy to silver-based small molecules in vitro and superior in vivo efficacy in a murine *P. aeruginosa* acute lung infection model.[29,31] We first introduced SCKs in the 1990s to overcome the micellar dissociation and enhance the structural stability.[32] The cross-linking provides structural stability to polymeric micelles, maintains its size and shape, and improves the ability for chemical modification. The SCK nanoparticles offer a versatile platform for efficient delivery of antimicrobials. The unique micellar structure comprising a hydrophobic core and hydrophilic shell allows for the codelivery of two unique therapeutics.[33] Furthermore, the physicochemical properties and surface characteristics of SCK nanoparticles, including hydrophilicity, density, and porosity of the core and shell, can also be easily customized. For instance, the molecular weight and length of the amphiphilic polymeric chain are directly linked to the nanoparticle size and can be utilized to precisely tune the nanoparticle size.[34] The amphiphilic block terpolymer comprising the SCKs was designed and synthesized to provide unique characteristics, such as efficient loading of silver ions by reversible interactions to alkyne side-chain moieties as well as the ability to penetrate the thick mucus encountered in the lungs of CF patients.[30] These nanoparticles provide sustained release, shield the therapeutic from biological interactions, and can be localized at the infection site,[35] resulting in a reduction in number of doses as well as propensity for resistance acquisition.

Several groups have reported synergy with antimicrobials when used in combination with silver.[36] A tobramycin/silver combination at specific concentrations exerts synergistic antimicrobial activity against *P. aeruginosa* biofilms.[37] Thus combination therapeutic strategies demonstrate tremendous potential and have been employed with FDA-approved SoC antibiotics. However, such combinations need careful dose calibrations as well as efficient delivery systems to eliminate potential pitfalls of both therapeutics. To enhance the efficacy of silver, we performed a high-throughput screen to identify potential antimicrobials with activity against *P. aeruginosa* that may synergize with silver. We identified 4-epi-minocycline, previously considered an inactive metabolite of minocycline,[38,39] as a molecule with antimicrobial activity against *P. aeruginosa*. Minocycline is a broad-spectrum bacteriostatic agent that inhibits protein synthesis and demonstrates potent antimicrobial activity.[40,41] In addition, minocycline also exhibits favorable absorption and pharmacokinetic properties upon oral or intravenous administration.[42] Because of these favorable characteristics and potent antimicrobial activity against Gram-positive and Gram-negative bacteria, i.v. minocycline was reintroduced in 2009 as an alternative therapy to treat MDR bacterial infections.[43] Minocycline, including its i.v. formulation, has also been used as an alternative therapeutic against *Staphylococcus aureus* and MRSA,[43] which are commonly found bacteria in CF lungs. We have evaluated the antimicrobial activity of 4-epi-minocycline against clinical isolates of *P. aeruginosa* and MRSA obtained from CF patients. Furthermore, we evaluated the efficacy of the parent drug, minocycline, and have demonstrated comparable antimicrobial activity to 4-epi-minocycline. Next, we have investigated the potential synergistic activity of the silver/minocycline combination against *P. aeruginosa* and MRSA using checkerboard and end-point colony forming unit (CFU) determination assays. Finally, we expand upon previously reported nanoparticle formulations loaded with silver cations.[29] We have taken advantage of the unique design of these nanoparticles and leveraged our expertise to incorporate both minocycline (core) and silver (shell) with the goal of developing novel formulations that provide sustained release of two therapeutics and shield them from biological interactions. Thus, we have investigated the potential of a silver/minocycline combination as a next-generation antibiotic to combat the threats presented by MDR pathogens.

DOI: 10.1021/acs.molpharmaceut.8b01288
Mol. Pharmaceutics 2019, 16, 1606−1619

MATERIALS AND METHODS

Materials. We obtained 4-epi-minocycline (Chemos, Germany), minocycline hydrochloride (Sigma-Aldrich), silver acetate (Sigma-Aldrich), dimethyl sulfoxide (DMSO) (Sigma-Aldrich), Mueller Hinton (MH) broth (BD Difco), tryptic soy agar (TSA) plates (BD BBL), sheep blood agar plates (BD), 2,2′-(ethylenedioxy)bis(ethylamine) (Sigma-Aldrich), 1-[3′-(dimethylamino)propyl]-3-ethylcarbodiimide methiodide (Sigma-Aldrich). The Spectra/Por dialysis membranes (MWCO 6−8 kDa) were purchased from Spectrum Laboratories (Rancho Dominguez, CA). Nanopure water (18 MΩ·cm) was acquired by means of a Milli-Q water filtration system (Millipore, Bedford, MA).

Preparation of Drug Solutions. 4-Epi-minocycline was dissolved in DMSO, and minocycline hydrochloride was dissolved in autoclaved water (Milli-Q synthesis system; Millipore, Billerica, MA) to prepare stock solutions at a final concentration of 1.0 mg/mL and stored at −80 °C until use. A fresh stock solution of 1.0 mg/mL silver acetate was reconstituted in autoclaved water before each experiment.

Preparation and Characterization of aSCKs. In brief, a polyphosphoester-based anionic amphiphilic diblock copolymer was synthesized from poly(2-ethylbutyl phospholane)-*block*-poly(butynyl phospholane) by a "click"-type thiol−yne reaction with 3-mercaptopropanoic acid.[44,45] Then, the anionic diblock copolymers (623 mg, 2.08 mmol of acrylic acid) were suspended into nanopure water (60.0 mL) and sonicated for 10 min. The clear solution was stirred for another 1 h to obtain well-dispersed micelles, followed by the addition of a solution of 2,2′-(ethylenedioxy)bis(ethylamine) (EDDA, 46.1 mg, 0.311 mmol) dropwise in nanopure water (10.0 mL). The solution was allowed to stir for 1 h at room temperature. To this reaction mixture was added dropwise a solution of 1-[3′-(dimethylamino)propyl]-3-ethylcarbodiimide methiodide (EDCI, 204 mg, 0.687 mmol) in nanopure water (10.0 mL) via a syringe pump over 1 h. The reaction mixture was allowed to stir overnight at room temperature and was then transferred to presoaked dialysis membrane tubes (MWCO ca. 12−14 kDa) and dialyzed against nanopure water for 36 h in the cold room (4−8 °C) to remove small molecules. The purified anionic SCK (aSCK) solution was lyophilized into powder and kept in the freezer at −20 °C.

Silver Loading into aSCKs. In a typical experiment, aSCKs (250 mg) were dissolved in 25.0 mL of nanopure water and sonicated for 5 min. Silver acetate (100 mg) in 20.0 mL of nanopure water was added, and the mixture solution was shaded with aluminum foil and stirred overnight. The solution was transferred to a centrifugal filter device (100 kDa MWCO) and washed extensively for several cycles (n > 3) with nanopure water to remove free small molecules. The purified samples were lyophilized and stored at −20 °C. The amount of silver loaded into the micelles was quantified by ICP−MS using rhodium as an internal standard. The drug loading efficiency was determined to be 28%, with a 10.1% silver loading (mass of silver/total mass of drug-loaded aSCKs).

Minocycline Loading into aSCKs. In a typical experiment, aSCKs (5.0 mg) were dissolved in 3.0 mL of nanopure water and sonicated for 5 min. Minocycline hydrochloride (1.5 mg) in 1.0 mL of nanopure water was added, and the mixture solution was shaded with aluminum foil and stirred overnight. The solution was transferred to a centrifugal filter device (100 kDa MWCO) and washed extensively for several cycles (n > 3) with nanopure water to remove free small molecules. The purified samples were lyophilized and stored at −20 °C. The amount of minocycline hydrochloride loaded into the micelles was quantified by UV−vis using absorbance at 345 nm. The drug-loading efficiency was determined to be 40%, with a 10.8% minocycline hydrochloride loading (mass of minocycline hydrochloride/total mass of drug-loaded aSCKs).

Dual Loading into aSCKs. In a typical experiment, Ag-loaded aSCKs (9.2 mg, containing 0.92 mg silver) were dissolved in 5.0 mL of nanopure water and sonicated for 5 min. Minocycline hydrochloride (2.8 mg) in 1.8 mL of nanopure water was added, and the mixture solution was shaded with aluminum foil and stirred overnight. The solution was transferred to a centrifugal filter device (100 kDa MWCO) and washed extensively for several cycles (n > 3) with nanopure water to remove free small molecules (Figure S2). The purified samples were lyophilized and stored at −20 °C. The amount of minocycline hydrochloride loaded into the micelles was quantified by UV−vis using absorbance at 345 nm, whereas the amount of silver loaded into the micelles was quantified by ICP−MS using rhodium as an internal standard. The drug-loading efficiency for minocycline hydrochloride was determined to be 51%, with a 13.4% minocycline hydrochloride loading (mass of minocycline hydrochloride/total mass of drug-loaded aSCKs).

Release of Drugs from Nanoparticles. The release profiles of the drug-loaded aSCKs were studied by monitoring the decrease in drug concentration over time in dialysis cassettes by ICP−MS or UV−vis. In a typical procedure, drug-loaded aSCKs (3.0 mL) were transferred into a presoaked dialysis cassette. The cassette was allowed to stir in a beaker containing 3000 mL of nanopure water at 37 °C. Aliquots (ca. 0.05 mL) were taken at predetermined time points up to 50 h. Silver and minocycline hydrochloride concentrations were determined by ICP−MS and UV−vis, respectively. The release experiments were conducted in triplicate.

Bacterial Culture. Clinical isolates of *P. aeruginosa* (PA0531, PA0540, PA0545, PA0551, PA0552, PA0554, PA0557, PA0561, PAHP3, PAM57-15, and PAO1) were streaked from frozen stocks onto TSA plates and incubated overnight at 37 °C. A single bacterial colony was then suspended in MH broth and allowed to grow at 37 °C in a shaking incubator at 200 rpm to an OD_{650} of 0.4, which corresponds to ∼5×10^8 CFU/mL. Bacterial cultures were adjusted to 5×10^5 CFU/mL to prepare a working stock for all experiments.

High-Throughput Screen. *P. aeruginosa* strain PAO1 was streaked onto lysogeny broth (LB) agar plates and incubated overnight at 37 °C. A single bacterial colony was resuspended in LB broth and grown overnight at 37 °C in a shaking incubator at 200 rpm. Compounds from the "SAC1" Sacchettini lab diversity library (∼50 000 unique compounds assembled in house; 1 mM in 100% DMSO) were transferred to clear 384-well assay plates (1.5 μL). The overnight culture was then diluted to an OD_{600} of 0.005 in fresh LB and aliquoted to assay plates (60 μL). Following a 2 h incubation at 37 °C, 0.2 μM filtered resazurin dye (0.05% w/v) was added (3 μL). After an additional hour of incubation, the absorbance at 573 and 605 nm was measured on a POLARstar Omega plate reader. The percent inhibition of each compound was calculated according to the following equation: % growth = $(\omega - \overline{xp})/(\overline{xn} - \overline{xp}) \times 100\%$, where values of ω (sample), p (positive control), and n (negative control) were determined

DOI: 10.1021/acs.molpharmaceut.8b01288
Mol. Pharmaceutics 2019, 16, 1606−1619

by the difference between sample absorbance values (OD_{573} − OD_{605}). Trimethoprim (100 μM) and DMSO were used as positive and negative controls, respectively.

In Vitro Antimicrobial Activity. Minimum inhibitory and bactericidal concentrations (MIC and MBC) were determined according to the standard Clinical and Laboratory Standards Institute (CLSI) broth-microdilution method. In brief, 100 μL of working stock of bacterial suspension was added to each well (n = 3) containing 100 μL of silver acetate, 4-epi-minocycline, or minocycline solution in a 96-well plate. All solutions were composed of 95% MH broth and 5% (v/v) DMSO. Bacteria were incubated with 0.06, 0.13, 0.25, 0.5, 1, 2, 4, 8, 16, 32, 64, and 128 μg/mL minocycline or 4-epi-minocycline or 0.13, 0.25, 0.5, 1, 2, 4, 8, 16, and 32 μg/mL silver acetate at 37 °C for 18−24 h under static conditions. The final concentration of DMSO in the assay was 2.5% (v/v). The MIC was determined as the lowest concentration that did not show any signs of bacterial growth upon visual inspection. Finally, the MBC was determined by plating the bacterial solutions demonstrating growth inhibition on blood agar plates and recording the lowest concentration that resulted in no growth after an 18−24 h incubation at 37 °C. All experiments were performed in triplicate. The color codes indicate the drug resistance cutoffs for minocycline against *S. aureus*, as published by the CLSI. Green, yellow, and red indicate if a particular *S. aureus* isolate is susceptible, intermediate susceptible, or resistant to minocycline, respectively. A similar scale was adopted for *P. aeruginosa*.

Determination of Synergistic Drug Combinations. Four *P. aeruginosa* isolates (PA0540, PA0557, PAHP3, and PAO1) were selected based on their sensitivity to silver acetate and minocycline. The selection criteria included one strain from each of the following categories; sensitive to both drugs, resistant to both drugs, or sensitive to one drug and resistant to the other drug. Hence, we selected PAO1, which is sensitive to both drugs; PA0540, which is sensitive to silver acetate and resistant to minocycline; PAHP3, which is sensitive to minocycline and resistant to silver acetate; and PA0557, which is resistant to both drugs. A dynamic concentration scale based on the MIC and MBC values was used to determine the optimal ratio of synergistic concentrations between the two therapeutic agents. The final solutions were composed of 95% MH broth and 5% DMSO. A 100 μL working stock of bacterial suspension was incubated with a 100 μL of solution of therapeutic agents (n = 3) for 18 h at 37 °C. Final drug concentrations incubated with each bacterial isolate are mentioned in Table 1. Wells demonstrating bacterial growth inhibition were identified visually to determine a synergistic MIC. All experiments were performed in duplicate. To evaluate for potential synergy, the fractional inhibitory concentration (FIC) was calculated, as shown in eq S1 and defined in Table S1.

Table 1. Concentrations of Silver Acetate and Minocycline Hydrochloride Incubated with Select *P. aeruginosa* Isolates To Determine Synergistic Activity[a]

strain	silver acetate concentration (μg/mL)	minocycline HCl concentration (μg/mL)
PAO1	1, 2, 3, 4, and 6	1, 2, 4, 8, 16, and 32
PAHP3	2, 4, 6, 8, and 16	1, 2, 4, 8, 16, and 32
PA0540	1, 2, 3, 4, and 6	4, 8, 16, 32, 64, and 128
PA0557	2, 4, 6, 8, and 16	2, 4, 8, 16, 32, and 64

[a]Bacteria were incubated with a combination of each of the drugs at the following concentrations.

Determination of Bacterial Burden for Synergistic Drug Combinations. Potential synergy between combinations of silver acetate and minocycline against *P. aeruginosa* isolates PA0557 and PA0540 at a final concentration of 10^6 CFU/mL was determined using a 24 h end-point CFU study performed in triplicate. The concentrations of silver acetate tested against PA0557 were 1, 2, and 4 μg/mL, and the concentrations of minocycline tested were 2, 4, 8, and 16 μg/mL. Individual drugs served as controls. The concentrations of silver acetate tested individually against PA0557 were 1, 2, 4, 6, and 8 μg/mL, and the tested concentrations of minocycline alone were 4, 8, 16, 32, and 64 μg/mL. The concentrations of silver acetate tested against PA0540 were 0.13, 0.25, 0.5, and 1 μg/mL, and the concentrations of minocycline tested were 16, 32, and 64 μg/mL. Individual drugs served as controls. The concentrations of silver acetate tested individually against PA0540 were 0.13, 0.25, 0.5, and 1 μg/mL, and the tested concentrations of minocycline alone were 16, 32, and 64 μg/mL. Synergy was defined as ≥2 $\log_{10}$ CFU/mL reduction between combined agents and the most effective individual agent at 24 h.[46]

The bacterial concentrations (CFU) of PA0557 were also determined after incubation with combinations of free drugs, as well as dual-loaded nanoparticles. Individual drugs at concentrations corresponding to those tested in combination as well as blank nanoparticles served as controls. The ratio of silver acetate to minocycline was maintained at 1:0.87 (w/w) for all combinations to mirror the drug loading in the dual-loaded nanoparticles. The tested concentrations of silver acetate and minocycline were 1, 2, 4, 6, and 8 μg/mL and 0.87, 1.74, 3.48, 5.22, 6.96 μg/mL, respectively. A 100 μL working stock of bacterial suspension was incubated with 100 μL of drug solution (n = 4) in each well of a 96-well plate at 37 °C for 24 h with constant shaking at 100 rpm. The final solutions were composed of 97.5% MH broth and 2.5% (v/v) DMSO. Finally, a 10-fold serial dilution was performed in MH broth with the bacterial suspension from each well, and 50 μL of each dilution was plated onto a blood agar plate. Plates were incubated for 18 h, and colonies were counted to determine the CFU for each condition. The potential synergistic effects between silver acetate and minocycline were determined as described above. All experiments were performed in duplicate.

Transmission Electron Microscopy. The drug-loaded nanoparticles suspended in aqueous solutions (4 μL) were deposited onto carbon-coated copper grids for 1 min, and excess solution was wicked away with a piece of filter paper. For minocycline-loaded SCKs, a drop of 1 wt % uranyl acetate was then added and allowed to stand for 30 s before the excess stain was wicked away. No stain was used for silver-loaded SCKs and dual-loaded SCKs. The grids were allowed to dry in air overnight. Transmission electron microscopy (TEM) images were collected using a JEOL 1200 EX electron microscope operating at 100 kV, and micrographs were recorded at calibrated magnifications using a SIA-15C charge-coupled device (CCD) camera.

Untreated bacteria and bacteria treated with silver acetate, minocycline, or both drugs, to be examined by TEM, were pelleted and fixed in 2.5% glutaraldehyde and 1% acrolein in 0.2 M Sorensen's phosphate buffer for 1 h at room temperature. The fixed samples were stained with 1% aqueous

DOI: 10.1021/acs.molpharmaceut.8b01288
Mol. Pharmaceutics 2019, 16, 1606−1619

osmium tetroxide overnight at 4 °C. Samples were dehydrated with acetone and then infiltrated with resin. Subsequently, the samples were thin-sectioned in a microtome (Boeckeler MTX), poststained in uranyl acetate and lead citrate, and then visualized on a JEOL 1200 EX electron microscope.

Statistical Analysis. All statistics were calculated using JMP Pro 13 for Macintosh (SAS Institute, Cary, NC, www.jmp.com). Differences between the treatments were investigated by one-way ANOVA, followed by Tukey's multiple comparison test (95% confidence intervals). * indicates $p \leq 0.05$, ** indicates $p \leq 0.01$, *** indicates $p \leq 0.001$, and **** indicates $p \leq 0.0001$.

RESULTS

High-Throughput Screening Identified 4-Epi-minocycline as a Potent Inhibitor of *Pseudomonas aeruginosa*. To identify novel compounds with antipseudomonal activity for loading into aSCK nanoparticles, we screened a high-diversity library of small molecules (SAC1) for inhibition of the clinical *P. aeruginosa* isolate, PAO1. Plates with high control variability, as indicated by control z' scores >0.4, were removed from the resulting data set. Of the remaining 39 340 compounds, 9 hits were identified with >90% growth inhibition (Figure 1). The properties of 4-epi-minocycline, including its high antimicrobial activity against PAO1 (98% inhibition) and hydrophobicity known to enhance loading into the core−shell interface of the aSCK nanoparticles,[47−49] prompted the use of this inhibitor for further efficacy studies.

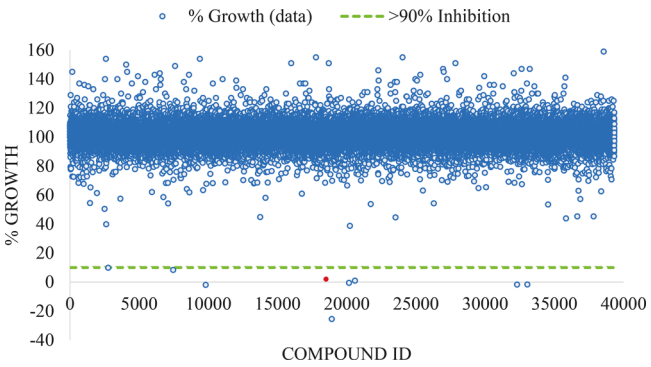

Figure 1. HTS bacterial inhibition screen. A small-molecule diversity library (SAC1) was screened for the inhibition of *P. aeruginosa* strain, PAO1. Nine compounds with >90% inhibition were identified. Of these potent inhibitors, 4-epi-minocycline was selected for characterization and downstream loading applications. 4-Epi-minocycline is highlighted in red. 10% growth (90% inhibition) cutoff is indicated by a dashed green line.

In Vitro Antimicrobial Activity of Silver Acetate, 4-Epi-minocycline, and Minocycline against *Pseudomonas aeruginosa*. We characterized the minimum inhibitory and bactericidal concentrations (MICs and MBCs) of 4-epi-minocycline, minocycline, and silver acetate against 11 *P. aeruginosa* clinical isolates (Table 2). Silver acetate has consistent antimicrobial activity against *P. aeruginosa*, with MICs between 4 and 6 μg/mL and MBCs between 4 and 8 μg/mL (Table 2). 4-Epi-minocycline exhibits MICs similar to those of minocycline against 8 of the 11 tested strains, whereas it shows slightly lower MICs than minocycline against the remaining 3 strains (Table 2). With regards to MBCs, 4-epi-minocycline exhibits MBCs against PA0554, PA0557, and PAM57-15 that are lower than those of minocycline, whereas the MBCs for 4-epi-minocycline and minocycline are comparable for PA0545 and PA0551. In contrast, minocycline has lower MBCs against PA0552, PAHP3, and PAO1 compared with 4-epi-minocycline. Finally, the MBCs of 4-epi-minocycline and minocycline are out of our detection range against PA0531 and PA0540 (Table 2).

Additive Effects of Silver Cations and Minocycline Demonstrated by Checkerboard Assay. To explore the potential synergistic antimicrobial effects between silver cations and minocycline, we tested combined drugs against four selected *P. aeruginosa* strains using a checkerboard assay. The MICs of combined drugs summarized in Table 3 are reduced compared with the MICs of silver cations or minocycline alone against PA0540, PA0557, and PAO1. However, on the basis of the FIC calculations performed using eq S1, we observe an additive effect for the combination of silver cations and minocycline rather than a synergistic effect against PA0540, PA0557, and PAO1. Interestingly, combining silver cations and minocycline did not change the MIC of either drug tested alone against PAHP3 (Table 3).

Synergistic Effects of Silver Cations and Minocycline Demonstrated by End-Point CFU Studies. Even though we did not observe a synergistic effect between silver cations and minocycline against *P. aeruginosa* using a checkerboard assay, we performed an end-point CFU study to investigate the effect of the combination therapeutic on CFU. The concentrations used in the 24 h end-point CFU study were selected based on the checkerboard assay result. For PA0557, the combinational MIC of silver acetate and minocycline is 2 and 4 μg/mL. For PA0540, the combinational MIC of silver acetate and minocycline is 1 and 32 μg/mL. Therefore, for the 24 h end-point CFU study, we selected silver acetate and minocycline concentrations at sub- or at individual MIC concentrations but included the combinational MIC within the testing range. The bacterial concentration of PA0557 is ~10^9 CFU/mL when treated with 4 μg/mL silver acetate or minocycline alone. However, following exposure to a combination of 4 μg/mL silver acetate and 2 μg/mL minocycline, the bacterial burden of PA0557 is reduced to <10^4 CFU/mL (Figure 2A,B). Because the synergistic effect in end-point CFU study is defined as a ≥2 $\log_{10}$ reduction in bacterial burden compared with the most efficacious individual treatment, the aforementioned combination of silver cations and minocycline demonstrated synergy in our end-point CFU study. We verified the synergy of this combination against an additional *P. aeruginosa* isolate, PA0540. Upon treatment with a combination of 0.5 μg/mL silver acetate and 32 μg/mL minocycline, PA0540 demonstrates a >2 $\log_{10}$ reduction of bacterial burden, indicating synergy (Figure 2C).

Characterization of the Nanoparticles. The anionic polymer was synthesized via thiol−yne reaction between 3-mercaptopropionic acid and diblock copolymer poly(2-ethyl-butoxy phospholane)-*block*-poly(2-butynyl phospholane) (PEBP-*b*-PBYP). Then, aSCKs were prepared by self-assembly of the anionic polymer, followed by cross-linking using a diamine as a cross-linker. Silver cations and minocycline were loaded into the aSCKs by mixing for 3 h and purified by centrifugal filter devices. In the absence of SCKs, most (>99.9%) of the free minocycline hydrochloride was removed after three washes (Figure S3). The dual-loaded aSCKs were obtained by stirring silver-loaded aSCKs with minocycline for 3 h, followed by purification. Both silver cations and

DOI: 10.1021/acs.molpharmaceut.8b01288
Mol. Pharmaceutics 2019, 16, 1606−1619

Table 2. MICs and MBCs of *Pseudomonas aeruginosa* Strains with Treatment of Silver Acetate, 4-Epi- minocycline, and Minocycline (units: μg/mL)

Drugs Names / *P.a.* Strains	Silver acetate		4-epi-minocycline		Minocycline	
	MIC	MBC	MIC	MBC	MIC	MBC
PAO1	4	4	4	64	4	64
PA0531	4	6	32	>128	32	>128
PA0540	4	6	32	>128	64	>128
PA0545	4	6	4	64	4	64
PA0551	4	6	8	64	8	64
PA0552	4	4	8	128	16	64
PA0554	4	6	8	64	8	128
PA0557	6	6	8	32	8	64
PA0561	4	6	16	>128	32	>128
PAHP3	4	8	8	32	8	32
PAM57-15	4	6	4	32	4	32

Drug Concentration	[drug]≤4	4<[drug]<16	[drug]≥16

Table 3. MIC of Combining Silver Acetate and Minocycline against Four Selected Strains of *Pseudomonas aeruginosa*

	drug		
strains	MIC (μg/mL) silver acetate/minocycline	FIC	FIC interpretation
PAO1	1/2	0.75	additive
PAHP3	4/8	2	indifference
PA0540	1/32	0.75	additive
PA0557	2/4	0.58	additive

minocycline could be loaded into the same aSCKs with ca. 10% loading (Table 4). Dual-loaded aSCKs had a slightly higher minocycline loading, which might be due to potential interactions between the two drugs. The sizes and size distributions of these silver- and minocycline-loaded nanoparticles were characterized by dynamic light scattering (DLS) and TEM (Figure 3). These data suggest that minocycline loading had little effect on the number-averaged hydrodynamic diameter of the nanoparticles. Previous studies have shown that the average diameter of the anionic micelles prior to cross-linking was 15 nm[30] and that after cross-linking was 16 nm

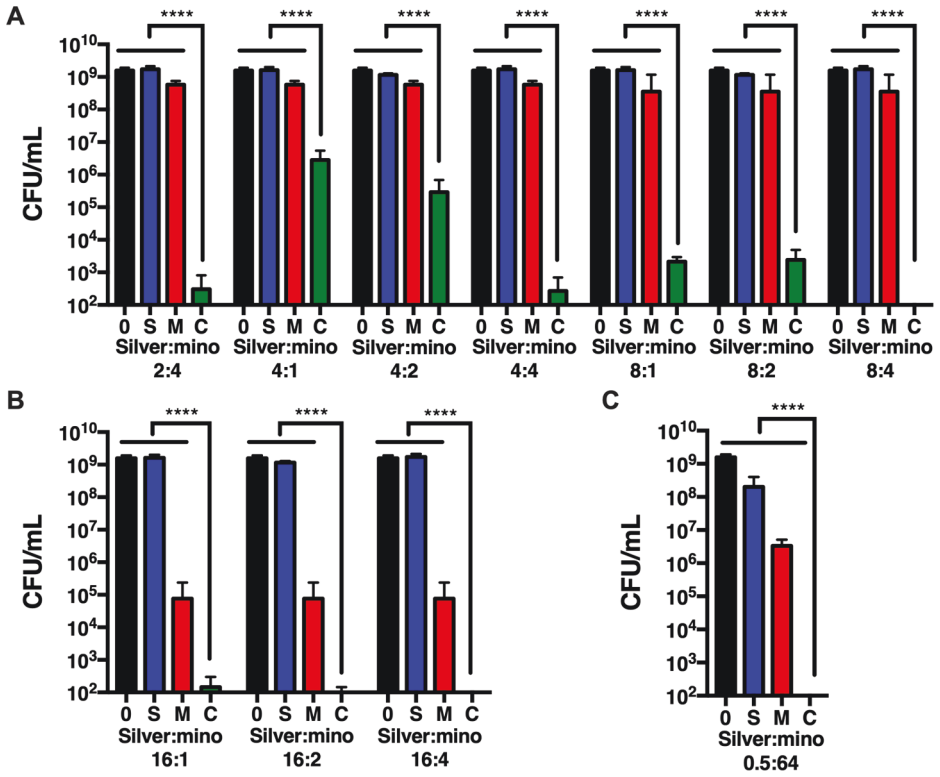

Figure 2. Synergy demonstrated between silver and minocycline against (A,B) PA0557 and (C) PA0540 by an end-point CFU study after 24 h of incubation with the drug concentration ratios (in μg/mL) indicated under each panel. 0: bacterial CFU without drug treatment; S: bacterial CFU treated with silver acetate; M: bacterial CFU treated with minocycline; C: bacterial CFU treated with silver acetate in combination with minocycline at the ratio indicated. Data are shown as mean and standard deviation (n = 6). Statistical significance determined by one-way ANOVA followed by Tukey's multiple comparison test (**** $p \leq 0.0001$).

DOI: 10.1021/acs.molpharmaceut.8b01288
Mol. Pharmaceutics 2019, 16, 1606−1619

Table 4. Silver and Minocycline Hydrochloride Loading into aSCKs

	compound loading			
drug-loaded SCKs	silver (mg)	minocycline hydrochloride (mg)	SCKs (mg)	drug loading (w/w %)
silver-loaded	0.464	0	4.6	10.1
minocycline-loaded	0	0.175	1.63	10.8
dual-loaded	0.161	0.217	1.62	Ag: 9.9; Mino:13.4

(D_{av} (TEM) = 16 ± 3 nm; D_h (DLS, number) = 16 ± 4 nm; D_h (DLS, volume) = 22 ± 14 nm; D_h (DLS, intensity) = 25 ± 8 nm).[35] The diameter of the silver-loaded nanoparticles was similar to that of empty nanoparticles, namely, 15 nm (Figure 3A; D_h (DLS, number) = 15 ± 4 nm; D_h (DLS, volume) = 19 ± 6 nm; D_h (DLS, intensity) = 175 ± 19 nm). The diameter of the minocycline-loaded nanoparticles was also similar to that of empty nanoparticles, namely, 12 nm (Figure 3B; D_h (DLS, number) = 12 ± 3 nm; D_h (DLS, volume) = 17 ± 9 nm; D_h (DLS, intensity) = 42 ± 27 nm). In contrast, the dual-loaded nanoparticles were slightly larger than either of the single-loaded SCK nanoparticles at 22 nm (Figure 3C; D_h (DLS, number) = 22 ± 6 nm; D_h (DLS, volume) = 33 ± 21 nm; D_h (DLS, intensity) = 131 ± 103 nm).

To investigate the release of minocycline from loaded aSCKs, drug-loaded aSCKs were placed into dialysis tubing containing nanopure water (Figure 4). Rapid drug releases were observed for all drug-loaded aSCKs. Minocycline was released from the single-loaded SCK nanoparticles into nanopure water with a release half life ($t_{1/2}$) of 1.1 h. The release $t_{1/2}$ of silver from the single-loaded nanoparticles was slightly longer at 1.8 h. Interestingly, the $t_{1/2}$ of minocycline release from the single-loaded nanoparticles was the same as

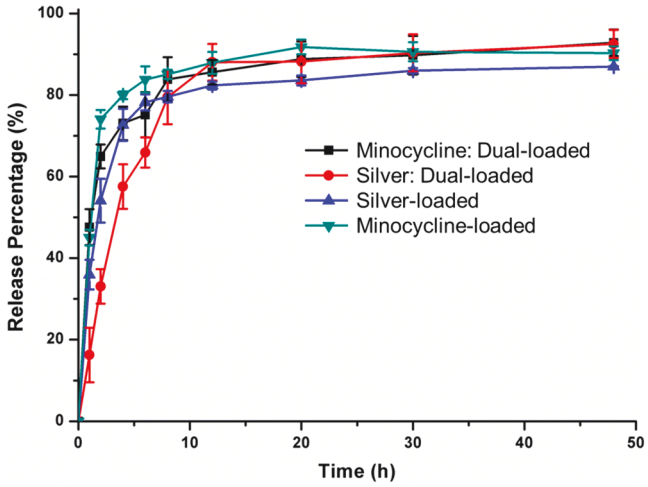

Figure 4. Release profiles of silver and minocycline from dialysis cassettes containing suspensions of silver-loaded, minocycline-loaded, or dual-loaded SCK nanoparticles at 37 °C in nanopure water. (Averages were calculated from triplicate experiments.)

that from the dual-loaded nanoparticles, but $t_{1/2}$ of silver release increased from 1.8 h for single-loaded nanoparticles to 3.4 h for dual-loaded nanoparticles, respectively (Figure 4, Table 5). In the absence of SCKs, ca. 90% of the free drug is released from the dialysis tubing within 1 h.

Silver and Minocycline Dual-Loaded Nanoparticles Demonstrated Efficacy against PA0557 and the Silver/Minocycline Ratio Demonstrated Synergy as Free Drugs in End-Point CFU Studies. In the previous experiments, silver acetate and minocycline were found to be synergistic as free drugs when the ratio between silver and minocycline was 2:1; however, this first iteration nanoparticle

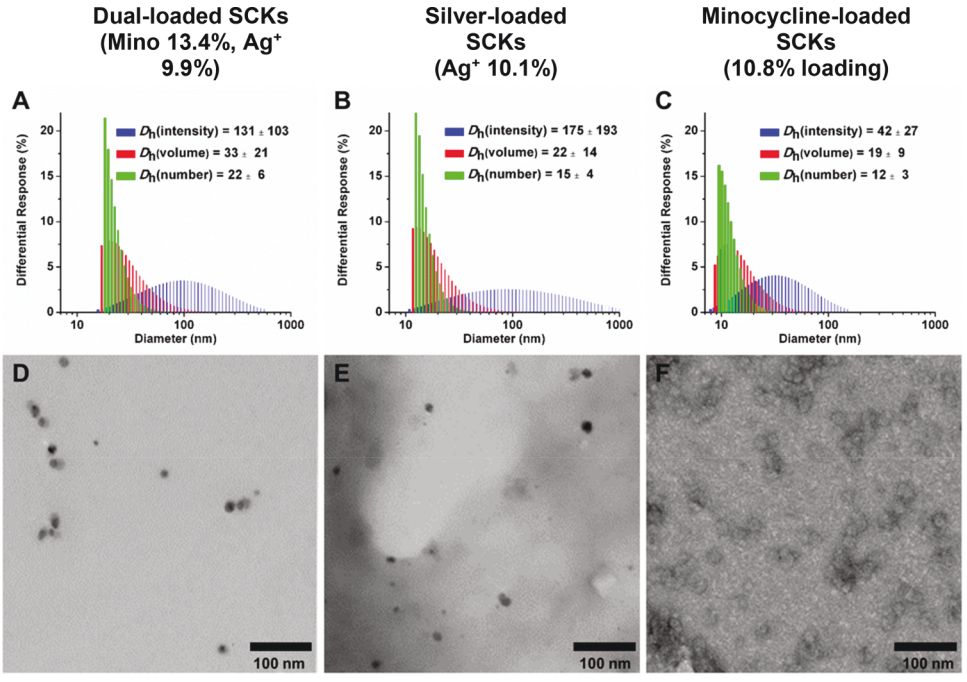

Figure 3. Characterization of nanoparticles. DLS histograms of intensity-averaged (D_h (intensity)), volume-averaged (D_h (volume)), and number-averaged (D_h (number)) hydrodynamic diameters of (A) dual-loaded, (B) Ag-loaded, and (C) minocycline-loaded SCK nanoparticles. Bright-field TEM images of (D) dual-loaded, (E) Ag-loaded, and (F) minocycline-loaded SCK nanoparticles. Minocycline-loaded SCKs were stained by uranyl acetate. Scale bar is 100 nm.

DOI: 10.1021/acs.molpharmaceut.8b01288
Mol. Pharmaceutics 2019, 16, 1606−1619

Table 5. Release Kinetics[a]

drug-loaded SCKs	drug release $t^{1/2}$	
	silver (h)	minocycline (h)
silver-loaded	1.8	NA
minocycline-loaded	NA	1.1
dual-loaded	3.4	1.1

[a]Release of minocycline and silver that was single- or dual-loaded into SCK nanoparticles at 37 °C in nanopure water, as measured by either ICP−MS (silver) or UV−vis (minocycline) in aliquots collected from the cassettes over 2 days.

formulation is loaded with a silver/minocycline ratio of 1.15:1, which provides a minocycline concentration of 3.48 μg/mL when the silver cation concentration is 4 μg/mL. The nanoparticles loaded with silver acetate alone or dual-loaded with silver acetate and minocycline demonstrated a 2 $\log_{10}$ or greater reduction in *P. aeruginosa* CFU compared with no treatment or empty nanoparticles when the silver acetate concentration was 4 μg/mL or higher (Figure 5A). Nanoparticles loaded with minocycline alone showed a 2 $\log_{10}$ or greater reduction in CFU compared with no treatment or empty nanoparticles when the minocycline concentration was 5.22 μg/mL or higher (Figure 5A). At the C3 concentration, treatment with dual-loaded nanoparticles resulted in a 5 $\log_{10}$ and a half-log reduction in bacterial burden compared with minocycline-loaded and silver-loaded nanoparticles, respectively. In contrast, when *P. aeruginosa* was treated with silver acetate and minocycline as free drugs at the same ratio found in the nanoparticles, the combination of 4 μg/mL silver acetate and 3.48 μg/mL minocycline was found to produce a >2 $\log_{10}$ reduction in CFU compared with either drug added alone and hence was synergistic (Figure 5B). The dual-loaded nanoparticles did not meet the definition of synergy at the C3 concentration because the antimicrobial effects of silver-loaded nanoparticles were significantly enhanced likely due to the sustained release of silver. Nevertheless, the dual-loaded nanoparticles demonstrated a 1/3 $\log_{10}$ further bacterial reduction compared with the same C3 concentrations of combined free drugs.

Transmission Electron Microscopy Demonstrated the Antimicrobial Activity of Silver Cations and Minocycline. In the absence of any treatment, *P. aeruginosa* showed typical cellular morphology with no damage to cellular components or membranes. When bacteria are exposed to silver cations at 4 μg/mL, electron-dense granules are observed along the bacterial membrane. An irregular morphology and disintegration of the cellular components is also seen. DNA condensation is also observed in the center of bacteria. Gaps are observed between the cytoplasm membrane and the cell wall. In the presence of 2 μg/mL minocycline, membrane segmentation is observed in *P. aeruginosa* along with condensed and disintegrated cellular components. Leakage of the cellular components from the bacterial cells is also observed. Gaps between the cytoplasm membrane and the cell wall are observed when bacteria are treated with minocycline. Finally, following the treatment of bacteria with both silver cations and minocycline, a combination of the previous observations, with silver deposition outside bacteria and segmentation of the bacterial membrane, resulting in leakage of bacterial components, is observed. In addition, electron-dense granules are seen in combination-treated bacteria but not with minocycline-treated bacteria (Figure 6).

DISCUSSION

The high rates of morbidity and mortality associated with MDR pathogens, in particular, MDR *P. aeruginosa*, pose a serious threat to the public health and call for the accelerated development of novel treatment strategies. Several new antimicrobial strategies are being evaluated by research laboratories across the world; however, to expedite the regulatory approval processes, we have focused on the development of combination therapies that utilize existing SoC antimicrobials. We have established antimicrobial efficacy of several silver-based small molecules.[29,50−53] Moreover, silver, incorporated into bandages or creams, has been widely used for the treatment of bacterial infections in burn and wound patients; however, the poor stability of these silver cations has limited its use in these topical applications. We have previously demonstrated the ability of nanoparticles to shield silver cations from such external factors and improve their bioavailability to address this limitation.[29] To further enhance the antimicrobial efficacy of silver against MDR pathogens as well as realize the full potential of SCK

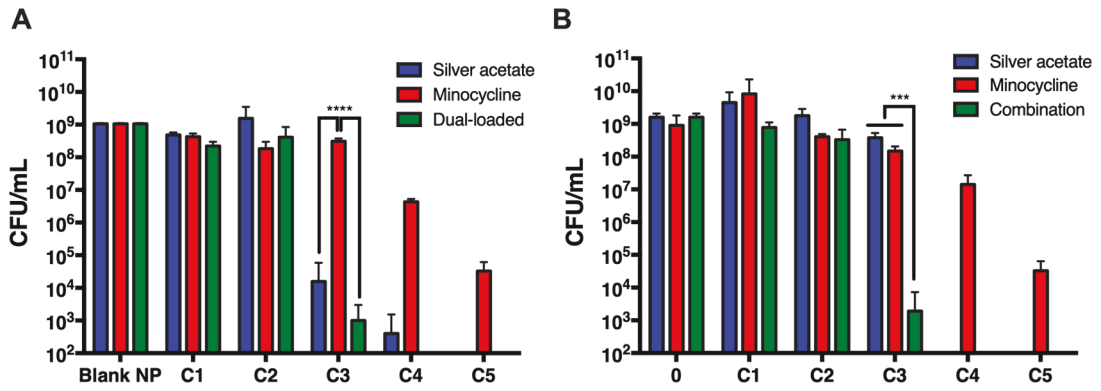

Figure 5. Silver and minocycline dual-loaded nanoparticles demonstrated efficacy against PA0557, and the combination of free silver and minocycline demonstrated synergy in end-point CFU studies. Colony counts of PA0557 after treating with (A) silver nanoparticles, minocycline nanoparticles, and dual-loaded nanoparticles and (B) free drug of silver and minocycline or silver combined with minocycline corresponding to the ratio of drugs found in the nanoparticles. The silver/minocycline concentrations tested were C1, 1:0.87; C2, 2:1.74; C3, 4:3.48; C4, 6:5.22; and C5, 8:6.96 μg/mL. Statistical significance determined by one-way ANOVA, followed by Tukey's multiple comparison test (*** $p \leq 0.001$, **** $p \leq 0.0001$).

DOI: 10.1021/acs.molpharmaceut.8b01288
Mol. Pharmaceutics 2019, 16, 1606−1619

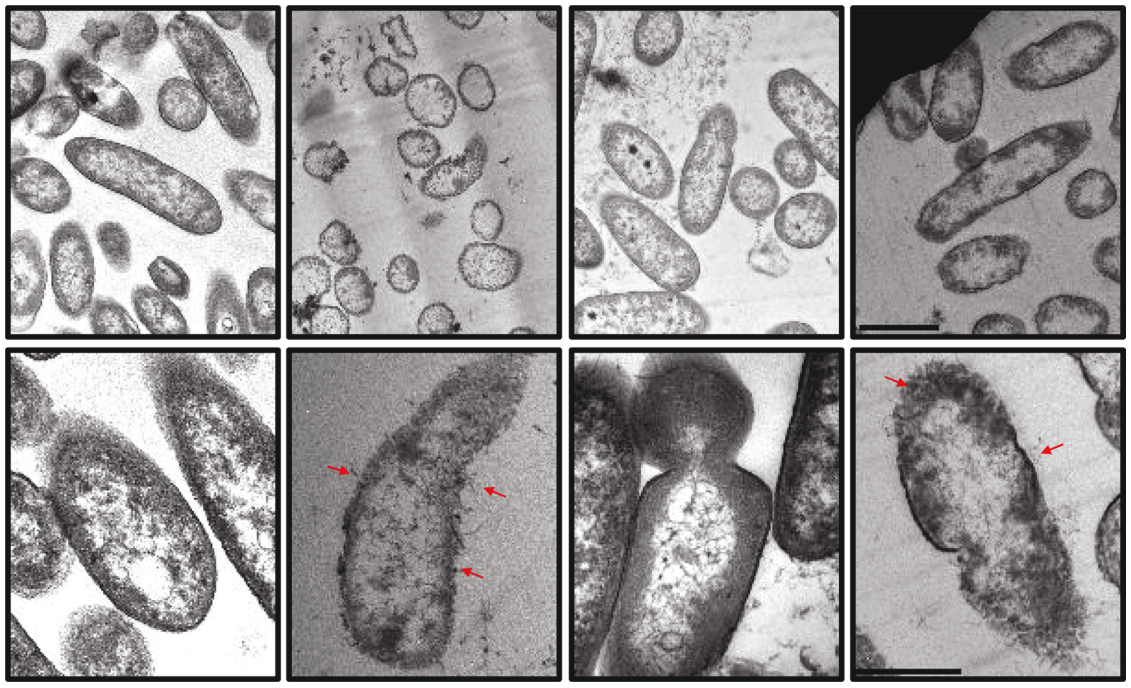

Figure 6. TEM images of *P. aeruginosa* treated with silver acetate, minocycline, or both. Top: *P. aeruginosa* strain PA0557 at 7.5k magnification (scale bar: 1 μm). Bottom: PA0557 at 20k magnification (scale bar: 0.5 μm). From left to right: without treatment; 4 μg/mL of silver acetate alone; 2 μg/mL of minocycline alone; and 4 μg/mL of silver acetate combined with 2 μg/mL of minocycline. Arrows indicate electron-dense granules outside bacteria and segmentation of the bacterial membrane.

nanoparticles, we selected 4-epi-minocycline as the candidate for combination therapy identified from the high-throughput screening of a diverse compound library. The hydrophobic nature of 4-epi-minocycline allows us to incorporate it in the core−shell interfaces of the SCK nanoparticles via hydrophobic interaction and electrostatic interaction between amino groups of the drug and carboxylate groups in the hydrophilic shells in conjunction with the silver cations loaded into the shell via electrostatic interaction with carboxylate groups and coordination with two sulfur atoms.[47−49,54] In addition, minocycline, an isomer of 4-epi-minocycline, is an SoC antimicrobial with potent antimicrobial activity against Gram-positive pathogens including MRSA. Thus minocycline and its isomers, including 4-epi-minocycline, are ideal candidates for use as combination therapeutics.

Minor structural differences between the parent compound, minocycline, and its isomer, 4-epi-minocycline, prompted further investigation into the activity of minocycline against these *P. aeruginosa* and MRSA isolates. Minocycline and 4-epi-minocycline demonstrate comparable antimicrobial activity against the 11 *P. aeruginosa* strains tested (Table 2). In addition, minocycline demonstrates comparable or superior antimicrobial activity to 4-epi-minocycline against 11 MRSA strains tested (Table S3). This observed activity of minocycline is comparable to previously reported results;[55] however, this is the first report of antimicrobial activity of 4-epi-minocycline, which is generally thought to be a pharmacologically inactive molecule.[56−58] The tetracycline family, including minocycline, inhibits protein synthesis through binding via its hydrophilic surface to the 16S rRNA component of the 30S ribosomal subunit.[59] A competition study has demonstrated that minocycline binds to the ribosomes in a fashion similar to tetracycline.[60] Hence, owing to the structural similarities between minocycline and 4-epi-minocycline exerts, we believe that 4-epi-minocycline exerts antimicrobial activity via a mechanism similar to that of tetracycline and minocycline.

Silver, on the contrary, demonstrated lower MIC values, namely, 4 μg/mL for seven of eight strains and 6 μg/mL for another, compared with the MICs of both 4-epi-minocycline and minocycline, which were 4 μg/mL for only three of eight strains and ranged from 8 to 32 μg/mL for the remaining five *P. aeruginosa* strains (Table 2). Furthermore, silver demonstrated relatively higher MIC values: MIC of 8 μg/mL against SAEH 05, MIC of 16 μg/mL against 4 of 11 tested MRSA strains, and 24 μg/mL against 6 of 11 tested MRSA strains (Table S3). This antimicrobial activity of silver is in agreement with previous reports.[30,61] These compounds have been evaluated individually as antimicrobial agents; however, their combinations with other antimicrobials have yet to be explored as next-generation antimicrobials. Minocycline has been used by clinicians as a broad-spectrum antibiotic with well-established pharmacokinetics, pharmacodynamics, efficacy, and safety profiles.[62,63] In addition, minocycline is known to epimerize into 4-epi-minocycline under mildly acidic conditions in the body and is excreted as a metabolite.[38,39] Moreover, minocycline demonstrated similar or superior antimicrobial efficacy to 4-epi-minocycline against tested *P. aeruginosa* and MRSA isolates *in vitro*. Finally, 4-epi-minocycline is an impurity isolated during the synthesis of minocycline. Thus the costs associated with synthesis, isolation, and purification of this epimer are significantly higher compared with minocycline. These parameters favored the use of minocycline over 4-epi-minocycline as the choice of drug for investigation in combination with silver.

A checkerboard assay was performed with four *P. aeruginosa* and four MRSA isolates, selected based on the MICs of silver and minocycline, to identify the optimal ratio of the two drugs that delivers maximum therapeutic efficacy. FIC values were

DOI: 10.1021/acs.molpharmaceut.8b01288
Mol. Pharmaceutics 2019, 16, 1606−1619

calculated[46] to identify synergistic or additive concentrations. The FIC values suggest additive effects for silver and minocycline ($0.5 < FIC \leq 1.0$) for three of the four tested strains of *P. aeruginosa* and all four tested MRSA strains (Table 3 and Table S5). However, the poor sensitivity of the checkerboard assay, which relies on evaluating turbidity in each microdilution to detect bacteriostatic effects, is a major limitation of the assay. A time-kill analysis defined by the CLSI was used to confirm synergy.[46] At 24 h, >2 $\log_{10}$ reduction in the bacterial burden with both *P. aeruginosa* isolates compared with individual treatments demonstrates synergy[64] between silver and minocycline (Figure 2). Furthermore, when combined with silver acetate, the required amount of minocycline reduced from 64 to 32 μg/mL against minocycline-resistant strain PA0540 to achieve synergistic effects (Figure 2C). We have confirmed similar results with MRSA isolates SAEH 05 and MRSA 0608 (Figure S1). SAEH 05, upon treatment with a combination of 4 μg/mL silver acetate and 0.13 μg/mL minocycline, demonstrates a >2 $\log_{10}$ reduction compared with individual drug treatments, indicating synergy (Figure S1A). Despite the significant reduction in the bacterial burden of MRSA 0608 treated with a combination of 2 μg/mL silver acetate and 0.5 μg/mL minocycline compared with individual drug treatments, the reduction is <2 $\log_{10}$, which does not meet the synergy criterion established by CLSI (Figure S1B). Thus although we observed a significant difference in the bacterial burden between the combination-treated group and the individual drug-treated groups, we did not identify synergistic effects between silver acetate in combination with minocycline against MRSA 0608 (Figure S1B). We speculate that given the relatively higher MICs of silver acetate against MRSA, the potent activity of minocycline as an anti-staphylococcal drug eclipses the effect of the combination therapy.

TEM was further used to confirm the morphological changes in *P. aeruginosa* after exposure to the silver/minocycline combination. Upon incubation with silver, deposition and accumulation are observed throughout the cross section of the samples at low and high magnifications. When bacteria are treated with silver or a silver and minocycline combination, electron-dense granules are seen. The electron-dense granule clusters likely represent the deposition of silver at the outer bacterial membrane, as demonstrated by Sondi and Salopek-Sondi[65] and supported by Feng et al.[61] Similar to data reported by our group and others, silver-treated bacteria exhibit irregular cellular shape and ruptured membranes, leading to the leakage and efflux of cytoplasmic contents.[66,67] In addition to membrane rupture, minocycline-treated bacteria cells uniquely show spheroplasts in the lower magnification images, membrane segmentation, as well as condensation of the inner membrane and detachment from the outer membrane. Regardless of their targets, antibiotics that disrupt protein synthesis display unique cellular disruptions, which result in similar effects.[68−70] Upon treatment with a combination of silver and minocycline, the TEM images show a combination of morphological changes that can be attributed to one of the two therapeutics. As far as we are aware, we are the first group to document the effect of minocycline against *P. aeruginosa* through TEM images. The absence of such TEM images in the literature may be due to minocycline's common use as an anti-staphylococcal but not as an anti-pseudomonal therapeutic.

The combination of silver and minocycline demonstrates tremendous potential as a combination therapy; however, the low bioavailability of silver cations and the potential side effects of long-term minocycline dosing remain a concern.[61,71,72] These pitfalls can be addressed by the use of drug-delivery devices such as nanoparticles. For instance, nanoparticles can be delivered directly to the lung, the site for *P. aeruginosa* infections in CF patients, minimizing interactions between the therapeutic and other organs.[73] Previously, Shah et al.[29] have demonstrated that silver-loaded SCK nanoparticles achieve a 16-fold reduction in the amount of silver compared with free drug to attain a 60% survival advantage in an acute *P. aeruginosa* pneumonia model. Moreover, the silver-loaded SCK nanoparticles were delivered in two doses compared with five doses required for free drug over a period of 72 h. Thus such localized drug administration into the lung results in lower systemic toxicity and adverse effects, a reduction in the number of drug doses,[29] as well as improved patient adherence.[73]

Nanoparticles with diameter <1 μm penetrate deeper into the alveolar region,[74] whereas smaller particles with diameter <5 nm are typically cleared at a rapid pace from the lung by exhalation as well as extravasation into the bloodstream.[75] Currently, the common nanoparticle drug formulations for lung therapeutics have diameters <500 nm to avoid alveolar macrophage uptake.[75] We have engineered particles with diameters ranging between 12 and 22 nm. The average 3D mesh spacing in CF lung mucus is 230 ± 50 nm,[76] whereas the pore size of *P. aeruginosa* biofilms has been found to be between 100 and 500 nm.[77] The smaller nanoparticles engineered here have the potential to overcome the mucus- and biofilm-associated obstruction in CF patients as well as to avoid opsonization by alveolar macrophages. Thus by optimizing the nanoparticle size, we can achieve enhanced penetration into otherwise difficult to penetrate mucus and biofilm layers to achieve sustained release in close proximity to the bacteria hiding in these complex matrices.

Both silver and minocycline single-loaded nanoparticles demonstrate antimicrobial activity somewhat comparable to that of the corresponding free drug (Figure 5 and Figure S2). In particular, the activity of minocycline-loaded nanoparticles mirrors that of free minocycline against *P. aeruginosa*, but they are less active than free minocycline at the C2 concentration against MRSA. Silver-loaded nanoparticles, however, demonstrate a 5 $\log_{10}$ greater reduction in *P. aeruginosa* CFU compared with free drug at the C3 concentration, which can be attributed to the sustained release and protection of Ag^+ cations from chloride ions afforded by the nanoparticles. A similar but slightly attenuated effect is also observed with MRSA (Figure S2). The more potent response of the silver single-loaded nanoparticles against *P. aeruginosa*, compared with MRSA, is likely due to the lower antimicrobial efficacy of silver cations against MRSA.

This initial dual-loaded nanoparticle formulation exhibits silver and minocycline loading at a ratio of 1.15:1 (1:0.87) that does not match the target 1:2 silver/minocycline ratio that was identified as synergistic in the free-drug checkerboard assays. Nevertheless, the combination of free silver and minocycline at this ratio at the C3 concentration in the CFU studies demonstrates a >2 $\log_{10}$ reduction in bacterial burden compared with individual free drugs, meeting the definition for synergy against *P. aeruginosa* (Figure 5B). However, because nanoencapsulated silver proved significantly more efficacious against *P. aeruginosa* than free silver at the C3

DOI: 10.1021/acs.molpharmaceut.8b01288
Mol. Pharmaceutics 2019, 16, 1606−1619

concentration, the dual-loaded nanoparticle formulation did not meet the definition for synergy compared with single-loaded nanoparticles in the CFU studies. Although they do not meet the definition of synergy, the dual-loaded nanoparticles demonstrate superior antimicrobial efficacy compared with each of the single-loaded nanoparticles at the C3 concentration (Figure 5A) as well as the combination of free drugs at C3 concentrations against *P. aeruginosa* (Figure 5B). For MRSA, dual-loaded nanoparticles at the C2 concentration demonstrate a 2 $\log_{10}$ reduction in the bacterial burden compared with individual drug-loaded nanoparticles, meeting the definition for synergy (Figure S2A). This activity of the dual-loaded nanoparticles is similar to that of the combination of free drugs against MRSA, although at the C2 concentration, the antimicrobial activity of free minocycline, the more potent anti-staphylococcal antimicrobial, is greater than that of the nanoparticle formulation (Figure S2B).

Taken together, these results suggest that *in vitro* studies of free drugs, either individually or in combination, may not predict the *in vitro* activity of dual-loaded nanoparticles given the complexities of individual drug release from a dual-loaded nanoparticle formulation. Moreover, the advantages of sustained release in an *in vivo* setting cannot be readily replicated in a static, *in vitro* experiment. The in vitro advantages of nanoparticles are limited because the delayed release of encapsulated drugs leads to lower concentrations of free drug available for antimicrobial activity. Additionally, these tests only measure activity against planktonic bacteria. Nevertheless, these results may also suggest that the identification of a loading ratio of silver and minocycline that might prove to be synergistic against *P. aeruginosa* in dual-loaded nanoparticles may be achieved by combining silver-loaded nanoparticles with free minocycline, given that the activity of the minocycline in the dual-loaded system mirrored that of the free drug, whereas the activity of the encapsulated silver was significantly enhanced compared with that of free silver. Ultimately, the ability of these nanoparticles to provide sustained release of two distinct therapeutics, one amphiphilic and one hydrophilic, imparts tremendous potential for their use as delivery devices. The unique design and chemistry of these SCK nanoparticles allow tailoring of the surface characteristics as well as the relative sizes of the hydrophobic core and hydrophilic shell, which allows tuning of the loading and release rates of both therapeutics. These optimizations to achieve release rates of the two antimicrobials that match synergistic ratios will provide a strong foundation for the next set of experiments and may realize the full potential of these drug-delivery devices as next-generation antimicrobials.

CONCLUSIONS

We have demonstrated the ability of two known SoC antimicrobials to synergistically eradicate MDR *P. aeruginosa* and *S. aureus*. We have also demonstrated by TEM the ability of both drugs to act in conjunction. Furthermore, we successfully synthesized silver and minocycline dual-loaded nanoparticles and demonstrated improved antibacterial activity compared with the combination of silver and minocycline as free drugs at the same concentrations. The lower concentrations of therapeutics, site-specific delivery, and sustained release achieved with nanoparticle formulations also reduce the possibility of generating drug-resistant mutants and systemic toxicity and may improve patients' adherence.

ASSOCIATED CONTENT

Supporting Information

The Supporting Information is available free of charge on the ACS Publications website at DOI: 10.1021/acs.molpharmaceut.8b01288.

Definitions of synergy as determined by the checkerboard assay and the 24 h end-point CFU study; antimicrobial susceptibility of commonly used antibiotics against the tested *Pseudomonas aeruginosa* and MRSA strains; MICs and MBCs of MRSA strains treated with 4-epi-minocycline, minocycline, and silver acetate as well as the combination of silver acetate and minocycline; synergy demonstrated between silver and minocycline against MRSA by a 24 h end-point CFU study; end-point CFU counts of MRSA treated with nanoparticles and free drug; and a control study demonstrating the release of free drug from the remaining minocycline hydrochloride concentration in the Centricon after washing and release of free minocycline from dialysis cassettes (PDF)

AUTHOR INFORMATION

Corresponding Authors

*E-mail: sacchett@tamu.edu (J.C.S.).
*E-mail: wooley@chem.tamu.edu (K.L.W.).
*E-mail: cannon@medicine.tamhsc.edu. Tel: (979) 436-0868. Fax: (979) 845-3479 (C.L.C.).

ORCID

James C. Sacchettini: 0000-0001-5767-2367
Karen L. Wooley: 0000-0003-4086-384X
Carolyn L. Cannon: 0000-0002-2491-0389

Author Contributions

‖Q.C., K.N.S., and F.Z. contributed equally.

Notes

The authors declare no competing financial interest.

ACKNOWLEDGMENTS

We acknowledge financial support from the National Heart Lung and Blood Institute of the National Institutes of Health as a Program of Excellence in Nanotechnology (HHSN268201000046C) and the National Science Foundation (DMR-1309724 and DMR-1105304). The Welch Foundation is acknowledged for support through the W. T. Doherty-Welch Chair in Chemistry, grant no. A-0001. The Microscopy & Imaging Center at Texas A&M University is gratefully acknowledged. The Johns Hopkins Medical Pathology Laboratory is acknowledged for providing confirmation of bacterial species, and antimicrobial susceptibility testing. We thank Justin Smolen for his kind assistance with the coordination of the studies and Erika Delgado for her technical assistance with HTS compound screening.

REFERENCES

(1) Lister, P. D.; Wolter, D. J.; Hanson, N. D. Antibacterial-Resistant *Pseudomonas aeruginosa* Clinical Impact and Complex Regulation of Chromosomally Encoded Resistance Mechanisms. *Clin. Micro. Rev.* **2009**, *22* (4), 582−610.

(2) Centers for Disease Control and Prevention. *Antibiotic Resistance Threats in the United States, 2013*, 2013. https://www.cdc.gov/drugresistance/pdf/ar-threats-2013-508.pdf.

DOI: 10.1021/acs.molpharmaceut.8b01288
Mol. Pharmaceutics 2019, 16, 1606−1619

(3) Curran, C. S.; Bolig, T.; Torabi-Parizi, P. Mechanisms and Targeted Therapies for *Pseudomonas aeruginosa* Lung Infection. *Am. J. Respir. Crit. Care Med.* **2018**, *197* (6), 708−727.
(4) Cystic Fibrosis Foundation. *Cystic Fibrosis Foundation Patient Registry 2016 Annual Data Report*; Cystic Fibrosis Foundation: Bethesda, MD, 2017.
(5) Govan, J. R.; Deretic, V. Microbial pathogenesis in cystic fibrosis: mucoid *Pseudomonas aeruginosa* and *Burkholderia cepacia*. *Microbiol. Rev.* **1996**, *60* (3), 539−574.
(6) Lyczak, J. B.; Cannon, C. L.; Pier, G. B. Lung Infections Associated with Cystic Fibrosis. *Clin. Micro. Rev.* **2002**, *15* (2), 194−222.
(7) Singh, P. K.; Schaefer, A. L.; Parsek, M. R.; Moninger, T. O.; Welsh, M. J.; Greenberg, E. P. Quorum-sensing signals indicate that cystic fibrosis lungs are infected with bacterial biofilms. *Nature* **2000**, *407* (6805), 762−764.
(8) Qi, L.; Li, H.; Zhang, C.; Liang, B.; Li, J.; Wang, L.; Du, X.; Liu, X.; Qiu, S.; Song, H. Relationship between Antibiotic Resistance, Biofilm Formation, and Biofilm-Specific Resistance in *Acinetobacter baumannii*. *Front. Microbiol.* **2016**, *7*, 483.
(9) Blaser, J.; Stone, B. B.; Groner, M. C.; Zinner, S. H. Comparative study with enoxacin and netilmicin in a pharmacodynamic model to determine importance of ratio of antibiotic peak concentration to MIC for bactericidal activity and emergence of resistance. *Antimicrob. Agents Chemother.* **1987**, *31* (7), 1054−1060.
(10) Marier, J. F.; Brazier, J. L.; Lavigne, J.; Ducharme, M. P. Liposomal tobramycin against pulmonary infections of *Pseudomonas aeruginosa* a pharmacokinetic and efficacy study following single and multiple intratracheal administrations in rats. *J. Antimicrob. Chemother.* **2003**, *52* (2), 247−252.
(11) Jung, W. K.; Koo, H. C.; Kim, K. W.; Shin, S.; Kim, S. H.; Park, Y. H. Antibacterial Activity and Mechanism of Action of the Silver Ion in *Staphylococcus aureus* and *Escherichia coli*. *Appl. Environ. Microbiol.* **2008**, *74* (7), 2171−2178.
(12) Wright, J. B.; Lam, K.; Hansen, D.; Burrell, R. E. Efficacy of topical silver against fungal burn wound pathogens. *Am. J. Infect. Control* **1999**, *27* (4), 344−50.
(13) Pirnay, J.-P.; De Vos, D.; Cochez, C.; Bilocq, F.; Pirson, J.; Struelens, M.; Duinslaeger, L.; Cornelis, P.; Zizi, M.; Vanderkelen, A. Molecular Epidemiology of *Pseudomonas aeruginosa* Colonization in a Burn Unit: Persistence of a Multidrug-Resistant Clone and a Silver Sulfadiazine-Resistant Clone. *J. of Clin. Microbiol.* **2003**, *41* (3), 1192−1202.
(14) Silver, S. Bacterial silver resistance: molecular biology and uses and misuses of silver compounds. *FEMS Microbiol. Rev.* **2003**, *27* (2−3), 341−353.
(15) Li, X. Z.; Nikaido, H.; Williams, K. E. Silver-resistant mutants of *Escherichia coli* display active efflux of Ag+ and are deficient in porins. *J. Bacteriol.* **1997**, *179* (19), 6127−6132.
(16) Gupta, A.; Matsui, K.; Lo, J.-F.; Silver, S. Molecular basis for resistance to silver cations in *Salmonella*. *Nat. Med.* **1999**, *5* (2), 183−188.
(17) Moyer, C. A. Some effects of 0.5% silver nitrate and high humidity upon the illness associated with large burns. *J. Natl. Med. Assoc.* **1965**, *57* (2), 95−100.
(18) Silver, S.; Phung, L. T.; Silver, G. Silver as biocides in burn and wound dressings and bacterial resistance to silver compounds. *J. Ind. Microbiol. Biotechnol.* **2006**, *33* (7), 627−634.
(19) Melaiye, A.; Youngs, W. J. Silver and its application as an antimicrobial agent. *Expert Opin. Ther. Pat.* **2005**, *15* (2), 125−130.
(20) Kollef, M. H.; Afessa, B.; Anzueto, A.; et al. Silver-coated endotracheal tubes and incidence of ventilator-associated pneumonia: The nascent randomized trial. *JAMA* **2008**, *300* (7), 805−813.
(21) Kang, Y. O.; Jung, J. Y.; Cho, D.; Kwon, O. H.; Cheon, J. Y.; Park, W. H. Antimicrobial Silver Chloride Nanoparticles Stabilized with Chitosan Oligomer for the Healing of Burns. *Materials* **2016**, *9* (4), 215.
(22) Trujillo, N. A.; Oldinski, R. A.; Ma, H.; Bryers, J. D.; Williams, J. D.; Popat, K. C. Antibacterial effects of silver-doped hydroxyapatite thin films sputter deposited on titanium. *Mater. Sci. Eng., C* **2012**, *32* (8), 2135−2144.
(23) Zahedi, P.; Rezaeian, I.; Ranaei-Siadat, S.-O.; Jafari, S.-H.; Supaphol, P. A review on wound dressings with an emphasis on electrospun nanofibrous polymeric bandages. *Polym. Adv. Technol.* **2009**, *21* (2), 77−95.
(24) Swathy, J. R.; Sankar, M. U.; Chaudhary, A.; Aigal, S.; Anshup; Pradeep, T. Antimicrobial silver: an unprecedented anion effect. *Sci. Rep.* **2015**, *4*, 7161.
(25) Liau, S. Y.; Read, D. C.; Pugh, W. J.; Furr, J. R.; Russell, A. D. Interaction of silver nitrate with readily identifiable groups: relationship to the antibacterial action of silver ions. *Lett. Appl. Microbiol.* **1997**, *25* (4), 279−83.
(26) Caster, J. M.; Patel, A. N.; Zhang, T.; Wang, A. Investigational nanomedicines in 2016: a review of nanotherapeutics currently undergoing clinical trials. *Wiley Interdiscip Rev. Nanomed Nanobiotechnol* **2017**, *9* (1), e1416.
(27) Kamaly, N.; Xiao, Z.; Valencia, P.; Radovic Moreno, A.; Farokhzad, O. Targeted polymeric therapeutic nanoparticles: design, development and clinical translation. *Chem. Soc. Rev.* **2012**, *41* (7), 2971.
(28) Lakshminarayanan, R.; Ye, E.; Young, D. J.; Li, Z.; Loh, X. J. Recent Advances in the Development of Antimicrobial Nanoparticles for Combating Resistant Pathogens. *Adv. Healthcare Mater.* **2018**, *7*, No. 1701400.
(29) Shah, P. N.; Lin, L. Y.; Smolen, J. A.; Tagaev, J. A.; Gunsten, S. P.; Han, D. S.; Heo, G. S.; Li, Y.; Zhang, F.; Zhang, S.; Wright, B. D.; Panzner, M. J.; Youngs, W. J.; Brody, S. L.; Wooley, K. L.; Cannon, C. L. Synthesis, Characterization, and In Vivo Efficacy of Shell Cross-Linked Nanoparticle Formulations Carrying Silver Antimicrobials as Aerosolized Therapeutics. *ACS Nano* **2013**, *7* (6), 4977−4987.
(30) Zhang, F.; Smolen, J. A.; Zhang, S.; Li, R.; Shah, P. N.; Cho, S.; Wang, H.; Raymond, J. E.; Cannon, C. L.; Wooley, K. L. Degradable polyphosphoester-based silver-loaded nanoparticles as therapeutics for bacterial lung infections. *Nanoscale* **2015**, *7* (6), 2265−2270.
(31) Li, Y.; Hindi, K.; Watts, K. M.; Taylor, J. B.; Zhang, K.; Li, Z.; Hunstad, D. A.; Cannon, C. L.; Youngs, W. J.; Wooley, K. L. Shell crosslinked nanoparticles carrying silver antimicrobials as therapeutics. *Chem. Commun.* **2010**, *46* (1), 121−123.
(32) Thurmond, K. B.; Kowalewski, T.; Wooley, K. L. Water-Soluble Knedel-like Structures: The Preparation of Shell-Cross-Linked Small Particles. *J. Am. Chem. Soc.* **1996**, *118* (30), 7239−7240.
(33) Qi, K.; Ma, Q.; Remsen, E.; Clark, C. G.; Wooley, K. Determination of the Bioavailability of Biotin Conjugated onto Shell Cross-Linked (SCK) Nanoparticles. *J. Am. Chem. Soc.* **2004**, *126* (21), 6599−6607.
(34) Thurmond, K. B.; Kowalewski, T.; Wooley, K. Shell Cross-Linked Knedels: A Synthetic Study of the Factors Affecting the Dimensions and Properties of Amphiphilic Core-Shell Nanospheres. *J. Am. Chem. Soc.* **1997**, *119* (28), 6656−6665.
(35) Elsabahy, M.; Wooley, K. Design of polymeric nanoparticles for biomedical delivery applications. *Chem. Soc. Rev.* **2012**, *41* (7), 2545.
(36) Niemirowicz, K.; Piktel, E.; Wilczewska, A. Z.; Markiewicz, K. H.; Durnas, B.; Watek, M.; Puszkarz, I.; Wroblewska, M.; Niklinska, W.; Savage, P. B.; Bucki, R. Core-shell magnetic nanoparticles display synergistic antibacterial effects against *Pseudomonas aeruginosa* and *Staphylococcus aureus* when combined with cathelicidin LL-37 or selected ceragenins. *Int. J. Nanomed.* **2016**, *11*, 5443−5455.
(37) Habash, M. B.; Goodyear, M. C.; Park, A. J.; Surette, M. D.; Vis, E. C.; Harris, R. J.; Khursigara, C. M. Potentiation of Tobramycin by Silver Nanoparticles against *Pseudomonas aeruginosa* Biofilms. *Antimicrob. Agents Chemother.* **2017**, *61* (11), No. e00415-17.
(38) Kelly, R. G.; Kanegis, L. A. Metabolism and tissue distribution of radioisotopically labeled minocycline. *Toxicol. Appl. Pharmacol.* **1967**, *11* (1), 171−183.
(39) Nelis, H. J.; De Leenheer, A. P. Metabolism of minocycline in humans. *Lancet* **1981**, *10* (2), 142−146.

DOI: 10.1021/acs.molpharmaceut.8b01288
Mol. Pharmaceutics 2019, 16, 1606−1619

(40) Bradford, P. A.; Jones, C. H. Tetracyclines. In *Antibiotic Discovery and Development*; Dougherty, T. J., Pucci, M. J., Eds.; Springer US: Boston, MA, 2012; pp 147−179.
(41) Brodersen, D. E.; Clemons, W. M., Jr.; Carter, A. P.; Morgan-Warren, R. J.; Wimberly, B. T.; Ramakrishnan, V. The structural basis for the action of the antibiotics tetracycline, pactamycin, and hygromycin B on the 30S ribosomal subunit. *Cell* **2000**, *103* (7), 1143−54.
(42) Jonas, M.; Cunha, B. A. Minocycline. *Ther. Drug Monit.* **1982**, *4* (2), 115.
(43) Colton, B.; McConeghy, K.; Schreckenberger, P.; Danziger, L. I.V. minocycline revisited for infections caused by multidrug-resistant organisms. *Am. J. Health-Syst. Pharm.* **2016**, *73* (5), 279−285.
(44) Zhang, S.; Zou, J.; Zhang, F.; Elsabahy, M.; Felder, S. E.; Zhu, J.; Pochan, D. J.; Wooley, K. L. Rapid and Versatile Construction of Diverse and Functional Nanostructures Derived from a Polyphosphoester-Based Biomimetic Block Copolymer System. *J. Am. Chem. Soc.* **2012**, *134* (44), 18467−18474.
(45) Zhang, S.; Li, A.; Zou, J.; Lin, L. Y.; Wooley, K. L. Facile Synthesis of Clickable, Water-Soluble, and Degradable Polyphosphoesters. *ACS Macro Lett.* **2012**, *1* (2), 328−333.
(46) Saiman, L. Clinical utility of synergy testing for multidrug-resistant *Pseudomonas aeruginosa* isolated from patients with cystic fibrosis: 'the motion for'. *Paediatr Respir Rev.* **2007**, *8* (3), 249−55.
(47) Baugher, A. H.; Goetz, J. M.; McDowell, L. M.; Huang, H.; Wooley, K. L.; Schaefer, J. Location of Fluorotryptophan Sequestered in an Amphiphilic Nanoparticle by Rotational-Echo Double-Resonance NMR. *Biophys. J.* **1998**, *75* (5), 2574−2576.
(48) Huang, H.; Wooley, K. L.; Schaefer, J. REDOR Determination of the Composition of Shell Cross-Linked Amphiphilic Core−Shell Nanoparticles and the Partitioning of Sequestered Fluorinated Guests. *Macromolecules* **2001**, *34* (3), 547−551.
(49) Kao, H.-M.; O'Connor, R. D.; Mehta, A. K.; Huang, H.; Poliks, B.; Wooley, K. L.; Schaefer, J. Location of Cholic Acid Sequestered by Core−Shell Nanoparticles Using REDOR NMR. *Macromolecules* **2001**, *34* (3), 544−546.
(50) Kascatan-Nebioglu, A.; Melaiye, A.; Hindi, K.; Durmus, S.; Panzner, M. J.; Hogue, L. A.; Mallett, R. J.; Hovis, C. E.; Coughenour, M.; Crosby, S. D.; Milsted, A.; Ely, D. L.; Tessier, C. A.; Cannon, C. L.; Youngs, W. J. Synthesis from Caffeine of a Mixed N-Heterocyclic Carbene−Silver Acetate Complex Active against Resistant Respiratory Pathogens. *J. Med. Chem.* **2006**, *49* (23), 6811−6818.
(51) Hindi, K. M.; Siciliano, T. J.; Durmus, S.; Panzner, M. J.; Medvetz, D. A.; Reddy, D. V.; Hogue, L. A.; Hovis, C. E.; Hilliard, J. K.; Mallet, R. J.; Tessier, C. A.; Cannon, C. L.; Youngs, W. J. Synthesis, Stability, and Antimicrobial Studies of Electronically Tuned Silver Acetate N-Heterocyclic Carbenes. *J. Med. Chem.* **2008**, *51* (6), 1577−1583.
(52) Kascatan-Nebioglu, A.; Panzner, M. J.; Tessier, C. A.; Cannon, C. L.; Youngs, W. J. N-Heterocyclic carbene−silver complexes: A new class of antibiotics. *Coord. Chem. Rev.* **2007**, *251* (5), 884−895.
(53) Cannon, C. L.; Hogue, L. A.; Vajravelu, R. K.; Capps, G. H.; Ibricevic, A.; Hindi, K. M.; Kascatan-Nebioglu, A.; Walter, M. J.; Brody, S. L.; Youngs, W. J. In Vitro and Murine Efficacy and Toxicity Studies of Nebulized SCC1, a Methylated Caffeine-Silver(I) Complex, for Treatment of Pulmonary Infections. *Antimicrob. Agents Chemother.* **2009**, *53* (8), 3285−3293.
(54) Lim, Y. H.; Tiemann, K. M.; Heo, G. S.; Wagers, P. O.; Rezenom, Y. H.; Zhang, S.; Zhang, F.; Youngs, W. J.; Hunstad, D. A.; Wooley, K. L. Preparation and in Vitro Antimicrobial Activity of Silver-Bearing Degradable Polymeric Nanoparticles of Polyphosphoester-block-Poly(l-lactide). *ACS Nano* **2015**, *9* (2), 1995−2008.
(55) Fujita, J.; Negayama, K.; Takigawa, K.; Yamagishi, Y.; Kubo, A.; Yamaji, Y.; Takahara, J. Activity of antibiotics against resistant *Pseudomonas aeruginosa*. *J. Antimicrob. Chemother.* **1992**, *29* (5), 539−546.
(56) Naidong, W.; Hua, S.; Roets, E.; Hoogmartens, J. Assay and purity control of minocycline by thin-layer chromatography using UV and fluorescence densitometry — a comparison with liquid chromatography. *J. Pharm. Biomed. Anal.* **1995**, *13* (7), 905−910.
(57) Heggie, W. Topical Formulation Containing a Tetracycline and a Method of Treating Skin Infections Using the Same. Patent WO2010149980A2, 2010.
(58) Sheth, N. V.; Valorose, J. J.; Ellway, K. A.; Ganesan, M. G.; Mooney, K. G.; Johnson, J. B. Pulsatile Once-a-Day Delivery Systems for Minocycline. U.S. Patent US5262173A, 2002.
(59) Nguyen, F.; Starosta, A. L.; Arenz, S.; Sohmen, D.; Donhofer, A.; Wilson, D. N. Tetracycline antibiotics and resistance mechanisms. *Biol. Chem.* **2014**, *395* (5), 559−75.
(60) Olson, M. W.; Ruzin, A.; Feyfant, E.; Rush, T. S., 3rd; O'Connell, J.; Bradford, P. A. Functional, biophysical, and structural bases for antibacterial activity of tigecycline. *Antimicrob. Agents Chemother.* **2006**, *50* (6), 2156−66.
(61) Feng, Q. L.; Wu, J.; Chen, G. Q.; Cui, F. Z.; Kim, T. N.; Kim, J. O. A mechanistic study of the antibacterial effect of silver ions on *Escherichia coli* and *Staphylococcus aureus*. *J. Biomed. Mater. Res.* **2000**, *52* (4), 662−668.
(62) Saivin, S.; Houin, G. Clinical Pharmacokinetics of Doxycycline and Minocycline. *Clin. Pharmacokinet.* **1988**, *15* (6), 355−366.
(63) Welling, P. G.; Shaw, W. R.; Uman, S. J.; Tse, F. L. S.; Craig, W. A. Pharmacokinetics of Minocycline in Renal Failure. *Antimicrob. Agents Chemother.* **1975**, *8* (5), 532−537.
(64) Petersen, P. J.; Labthavikul, P.; Jones, C. H.; Bradford, P. A. In vitro antibacterial activities of tigecycline in combination with other antimicrobial agents determined by chequerboard and time-kill kinetic analysis. *J. Antimicrob. Chemother.* **2006**, *57* (3), 573−576.
(65) Sondi, I.; Salopek-Sondi, B. Silver nanoparticles as antimicrobial agent: a case study on *E. coli* as a model for Gram-negative bacteria. *J. Colloid Interface Sci.* **2004**, *275* (1), 177−82.
(66) Kascatan Nebioglu, A.; Melaiye, A.; Hindi, K.; Durmus, S.; Panzner, M.; Hogue, L.; Mallett, R.; Hovis, C.; Coughenour, M.; Crosby, S.; Milsted, A.; Ely, D.; Tessier, C.; Cannon, C.; Youngs, W. Synthesis from Caffeine of a Mixed N-Heterocyclic Carbene−Silver Acetate Complex Active against Resistant Respiratory Pathogens. *J. Med. Chem.* **2006**, *49* (23), 6811−6818.
(67) Banasiuk, R.; Frackowiak, J. E.; Krychowiak, M.; Matuszewska, M.; Kawiak, A.; Ziabka, M.; Lendzion-Bielun, Z.; Narajczyk, M.; Krolicka, A. Synthesis of antimicrobial silver nanoparticles through a photomediated reaction in an aqueous environment. *Int. J. Nanomed.* **2016**, *11*, 315−324.
(68) Rodgers, F. G.; Tzianabos, A. O.; Elliott, T. S. The effect of antibiotics that inhibit cell-wall, protein, and DNA synthesis on the growth and morphology of *Legionella pneumophila*. *J. Med. Microbiol.* **1990**, *31* (1), 37−44.
(69) Klainer, A. S.; Russell, R. R. Effect of the inhibition of protein synthesis on the *Escherichia coli* cell envelope. *Antimicrob. Agents Chemother.* **1974**, *6* (2), 216−24.
(70) Peach, K. C.; Bray, W. M.; Winslow, D.; Linington, P. F.; Linington, R. G. Mechanism of action-based classification of antibiotics using high-content bacterial image analysis. *Mol. BioSyst.* **2013**, *9* (7), 1837−48.
(71) Holt, K. B.; Bard, A. J. Interaction of Silver(I) Ions with the Respiratory Chain of Escherichia coli: An Electrochemical and Scanning Electrochemical Microscopy Study of the Antimicrobial Mechanism of Micromolar Ag+. *Biochemistry* **2005**, *44* (39), 13214−13223.
(72) Smith, K.; Leyden, J. Safety of doxycycline and minocycline: A systematic review. *Clin. Ther.* **2005**, *27* (9), 1329−1342.
(73) Patton, J. S.; Byron, P. R. Inhaling medicines: delivering drugs to the body through the lungs. *Nat. Rev. Drug Discovery* **2007**, *6* (1), 67−74.
(74) Bailey, M. M.; Berkland, C. J. Nanoparticle formulations in pulmonary drug delivery. *Med. Res. Rev.* **2009**, *29* (1), 196−212.
(75) Lim, Y. H.; Tiemann, K. M.; Hunstad, D. A.; Elsabahy, M.; Wooley, K. L. Polymeric nanoparticles in development for treatment of pulmonary infectious diseases. *Wiley Interdiscip. Rev: Nanomed and Nanobiotechnol* **2016**, *8* (6), 842−871.

DOI: 10.1021/acs.molpharmaceut.8b01288
Mol. Pharmaceutics 2019, 16, 1606−1619

(76) Ensign, L. M.; Schneider, C.; Suk, J. S.; Cone, R.; Hanes, J. Mucus Penetrating Nanoparticles: Biophysical Tool and Method of Drug and Gene Delivery. *Adv. Mater.* **2012**, *24* (28), 3887−3894.
(77) Günday Türeli, N.; Türeli, A. E.; Schneider, M. Optimization of ciprofloxacin complex loaded PLGA nanoparticles for pulmonary treatment of cystic fibrosis infections: Design of experiments approach. *Int. J. Pharm.* **2016**, *515* (1), 343−351.

DOI: 10.1021/acs.molpharmaceut.8b01288
Mol. Pharmaceutics 2019, 16, 1606−1619